

SNEV is an evolutionarily conserved splicing factor whose oligomerization is necessary for spliceosome assembly

Johannes Grillari^{1,4,*}, Paul Ajuh², Guido Stadler¹, Marlies Löscher¹, Regina Voglauer¹, Wolfgang Ernst¹, Janet Chusainow², Frank Eisenhaber³, Marion Pokar¹, Klaus Fortschegger¹, Martin Grey⁵, Angus I. Lamond² and Hermann Katinger¹

¹Institute of Applied Microbiology, University of Natural Resources and Applied Life Sciences, Vienna, Austria Muthgasse 18, A-1190 Vienna, ²Division of Gene Regulation and Expression, Wellcome Trust Biocentre University of Dundee, Dow Street, DD15EH Dundee, UK, ³Institute of Molecular Pathology, Dr. Bohr-Gasse 7, A-1030 Vienna, Austria, ⁴BMT Research, Vienna, Austria and ⁵J.W. Goethe-University, Institute for Microbiology, Theodor-Stern-Kai 7, D-60590 Frankfurt am Main, Germany

Received September 13, 2005; Revised and Accepted November 11, 2005

ABSTRACT

We have isolated the human protein SNEV as down-regulated in replicatively senescent cells. Sequence homology to the yeast splicing factor Prp19 suggested that SNEV might be the orthologue of Prp19 and therefore might also be involved in pre-mRNA splicing. We have used various approaches including gene complementation studies in yeast using a temperature sensitive mutant with a pleiotropic phenotype and SNEV immunodepletion from human HeLa nuclear extracts to determine its function. A human–yeast chimera was indeed capable of restoring the wild-type phenotype of the yeast mutant strain. In addition, immunodepletion of SNEV from human nuclear extracts resulted in a decrease of *in vitro* pre-mRNA splicing efficiency. Furthermore, as part of our analysis of protein–protein interactions within the CDC5L complex, we found that SNEV interacts with itself. The self-interaction domain was mapped to amino acids 56–74 in the protein’s sequence and synthetic peptides derived from this region inhibit *in vitro* splicing by surprisingly interfering with spliceosome formation and stability. These results indicate that SNEV is the human orthologue of yeast PRP19, functions in splicing and that homooligomerization of SNEV in HeLa nuclear extract is essential for spliceosome assembly and that it might also be important for spliceosome stability.

INTRODUCTION

In our search for novel factors involved in the control of cellular life span *in vitro* we previously screened for genes that are differentially expressed in senescent versus early passage human umbilical vein endothelial cells (HUVECs) (1). From the identified genes we selected one, unknown gene 4, in order to test if it influences the replicative life span of HUVECs when overexpressed. Indeed, we observed that the transfected cells underwent more population doublings than the cells transfected with a control vector (2). Therefore, we termed the corresponding protein senescence evasion factor (SNEV). Sequence analysis of SNEV showed similarity to the *Saccharomyces cerevisiae* protein Prp19p/Pso4p/Xs9 (Figure 1), which has been identified independently by two different approaches: On the one hand it has been characterized as yeast Prp19p, a protein that is essential for splicing (3,4) and a subunit of the highly conserved nineteen complex (NTC), a complex consisting of several spliceosomal proteins (5–9).

On the other hand, studies within the field of DNA repair have identified it as Pso4p by complementation of the yeast strain pso4-1, a psoralen sensitive mutant (10). The phenotype of this yeast mutant strain is pleiotropic and comprises temperature sensitivity, mutagen and radiation sensitivity, a block of sporulation, impaired induced mutagenesis (11–13) as well as accumulation of pre-mRNA (14). These studies have provided a novel link between pre-mRNA processing and DNA repair (10,15) and suggest that Prp19p is involved in at least these two different and highly interesting cellular processes.

*To whom correspondence should be addressed. Tel: +43 1 36006 6231; Fax: +43 1 3697615; Email: j.grillari@iam.boku.ac.at

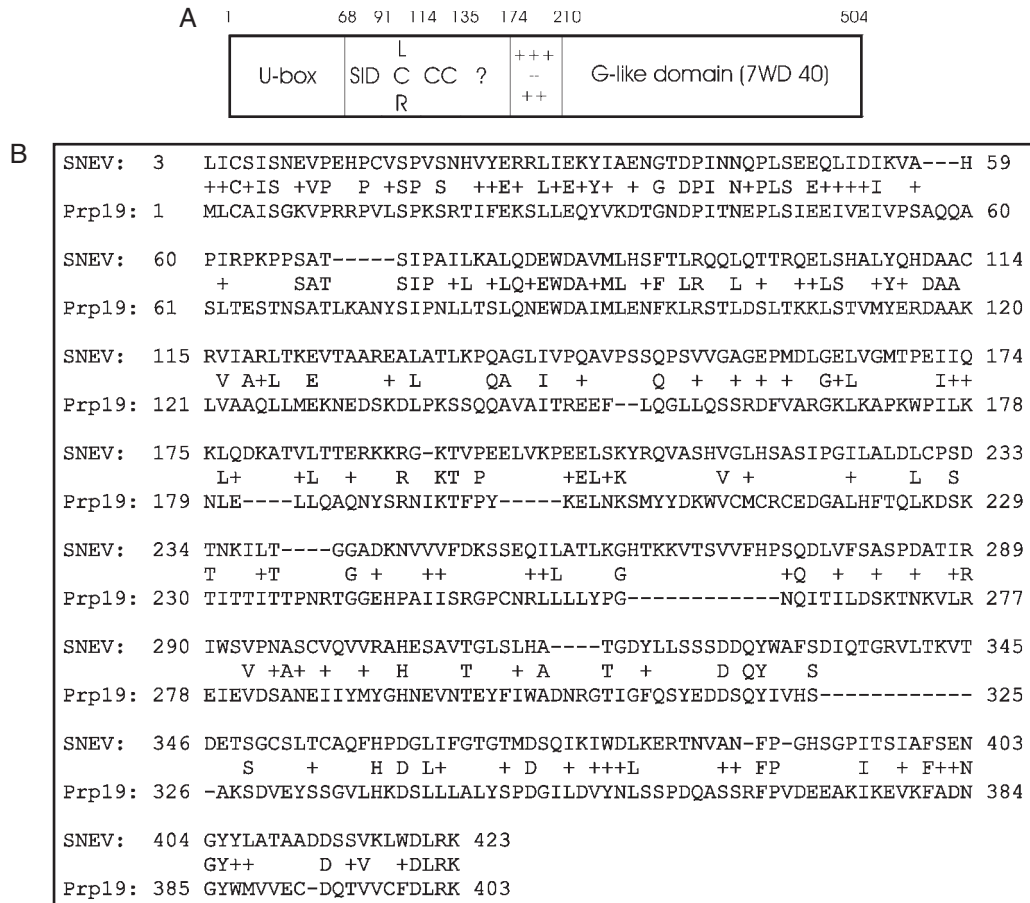


Figure 1. Sequence comparison of SNEV and Prp19p. (A) Domain architecture of human SNEV and yeast Prp19p is similar and consists of a UFD2 like box (U-box), a low complexity region (LCR), a coiled coil region (CC), a putative globular domain (?), as well as a charged region (+++--). (B) Alignment by BLAST shows 23% overall identities (423/504; 23% identities and 42% positives). Highest homology can be seen at the N-terminus, whereas the C-terminus differs.

Human SNEV, however, has been identified simultaneously to our studies as human nuclear matrix protein hNMP200 (16). Since it displays E3 ubiquitin ligase activity *in vitro* (17), it is highly probable that it is involved in the ubiquitin proteasome system *in vivo*. In line with this finding, we reported recently that it associates directly with the 20S proteasome, suggesting that it escorts its ubiquitinated (but still unknown) substrate(s) to the site of destruction (18).

In addition to these reports, SNEV has been found to be contained within the CDC5L complex by independent studies (19–21), a subspliceosomal complex containing highly similar proteins as the NTC complex in yeast.

During pre-mRNA splicing the non-coding intronic sequences of the nascent RNA transcripts of RNA polymerase II are removed and the coding exons are joined together to form mature mRNA within the cell nucleus. This mRNA is then exported for translation into the cytoplasm. The large complex that is responsible for this catalysis, the spliceosome, consists of many RNA and protein factors that assemble in a stepwise manner around the pre-mRNA before catalysis (22). Besides the RNA components that form four ribonucleoprotein (snRNP) particles (U1, U2, U5 and U4/6.U5), multiple non-snRNP associated proteins that are essential for spliceosome assembly and activity (23). One subcomplex

that seems highly conserved from yeast to human is the NTC (in yeast), or Prp19/CDC5L associated complex in human cells. The human complex is essential for the pre-mRNA splicing catalysis and consists of the core proteins CDC5L, SNEV/Prp19, Hsp73, PLRG1 and SPF27 (19,21). Dependent on the author of the experiments either AD002 and β -catenin-like 1 are found as members of the core complex (19,21) or CCAP6 (19). However, this complex is stably associated with the activated spliceosome as well as with a novel 35S form of the U5 snRNP (21), and depletion of this complex leads to block of the splicing reaction before the first catalytic step, during which the lariat is formed (21). Similarly, in yeast NTC is required for splicing catalysis (3), stable association of U5 and U6 with the spliceosome after U4 is dissociated and for a structural change in U6 snRNP (24). Furthermore, the NTC has recently been reported to be implicated in regulating the fidelity of splice site selection (25). Recruitment of the NTC to intron containing genes during transcription also supports the hypothesis that pre-mRNA splicing occurs co-transcriptionally (26).

Although SNEV has been found within the CDC5L/Prp19 complex, a direct role of SNEV in the human pre-mRNA splicing process has not been addressed so far and therefore

it is not clear yet, if SNEV is indeed the functional orthologue of Prp19p.

In this study we have addressed these questions by complementation studies in the *pso4-1* yeast mutant strain. Indeed, a human–yeast chimeric protein is able to restore the yeast wild-type phenotype. Additionally, we show that SNEV presence is required in human nuclear extracts for *in vitro* pre-mRNA splicing. Furthermore, we observed that formation of SNEV homo-oligomers is essential for the assembly of the spliceosome at a surprisingly early step. These results strongly suggest that SNEV is the orthologue of Prp19p and underline its multifaceted nature that seems to connect as distinct cellular functions as mRNA processing, protein degradation, DNA repair and replicative senescence.

MATERIALS AND METHODS

Protein sequence analysis

The protein sequences have been tested for the occurrence of low complexity regions with the SEG program (27) coiled coil segments (28), transmembrane regions (29), sequence compositional properties (30) and the occurrence of described globular domains from the PFAM (31) and SMART (32) databases. The existence of typical short structural repeats

was also tested with the REP tool (33). The remaining suspected globular protein segments have been subjected to iterative databases with the BLAST/PSI-BLAST tool (34).

Construction of plasmids and transformation into yeast

PCR, transformation of *Escherichia coli* cells, restriction reactions, DNA ligations and other recombinant DNA techniques were performed following standard protocols (35). In brief, the open reading frames (ORF) of Prp19 and SNEV were cloned into the yeast expression vector pYPGE15 under the control of the constitutive PGK promoter. For cloning of the chimeric proteins, the human and yeast gene parts were amplified by PCR and fused to a His₆-tag using primers carrying an asymmetric BpmI restriction site, that allowed seamless transition of human to yeast sequence (Table 1). The constructs were introduced into the yeast strain MG5128 (MATa/MAT α , *ura3-52/ura3*, *can1/CAN*, *pso4-1/pso4-1*) by LiAc transformation (36). Yeast clones were selected on media lacking uracil.

Furthermore, SNEV and truncated SNEV cDNAs were ligated into pGADT7 and pGBKT7 for yeast two hybrid analysis, into pEYFP-C1, pEYFP-N1, pECFP-C1 and pECFP-N1 for Fluorescence resonance energy transfer (FRET) analysis, (Clontech Laboratories, Palo Alto, USA) as well as into pGEX-6P-1 (Amersham Biosciences, Uppsala, Sweden) for glutathione *S*-transferase (GST)-fusion protein expression.

Table 1. Primers used in this study

Primer name	Sequence
Prp19 start sense	AattagcaattgcccaccATGCTTTGTGCTATTAGTGG
Prp19 stop as	GacgctcgagaacTTAGGGTGTCAATGCAACAATA
Prp19 stop as 6His	GacgctcgagaacctaataatgatgatgatgatgGGGTGTCAATGCAACAATATTG
SNEV start sense	AattagcaattgcccaccATGTCCCTAATCTGCTCCAT
SNEV stop as 6His	gacgctcgagaacctaataatgatgatgatgatgCAGGCTGTAGAACTTGAGGC
SNEV fastbac sense	gacggaattCTCGGTCCGAAACCATGTCCG
SNEV stop as	gacgctcgagaacCTACAGGCTGTAGAACTTGAG
SNEV Ubox as BpmI	ctttcactggagCCGGGATGCTGGTGGCTG
Prp19 wo Ubox sense BpmI	atcagctggagAGTCTACAACTCTGCTACG
Prp19 wo Ubox sense ATG	AattagcaattgcccaccatgGCTACGTTAAAAGCGAATTATTC
SNEV 273 as BpmI	atcatgctggagCGGGTTGTCTGCAGTgaGCCGAGAGTGA
Prp19 289 sense BpmI	aattagctggagCTTTAAGTTACGATCAACTCTAGATAG
Prp19 289 sense ATG	aattagcaattgcccaccatgTTACGATCAACTCTAGATAG
Prp19 291 as BpmI	atcatgctggagCTATCTAGAGTTGATCGTAAC
SNEV 264 sense BpmI	aattagctggagCAGCTTCACTCTGCGACAGCAGCT
Prp19 297 stop as	gacgctcgagaacctaataatgatgatgatgatgTCGTAACCTAAAAGTTTTCGAGC
SNEV 630 as BpmI	atcatgctggagCACCTGCCGGTATTTGCTG
Prp19 607 sense BpmI	AattagctggagTCTATGTAATATGAcAAATGGGTG
Prp19 622 sense ATG	aattagcaattgcccaccatgAAATGGGTGTGCATGTGTGTC
SNEV 1470 as BpmI	atcatgctggagCTTTAAGCTTGCGCAGATCCC
Prp19 1187 sense BpmI	aattagctggagTGGTTTGCTTTGACCTAAGAAAAG
Prp19 1198 sense ATG	AattagcaattgcccaccatgGACCTAAGAAAAGGATGTCGGC
PGK Promoter sense	CAAGATCTCGACTCTAGAGG
Cyc1 Terminator as	GCCTGTTTACTCACAGGC
SNEV 8 as new	AAGACTGTGCCTGAGGAGCTG
Prp19 503 sense	AGCTCAAAGCACCCAAATGG
SNEV sense	GTAGAATTCATGTCCCTAATCTGCTCCATC
SNEV antisense	ATACAAGTCGACCTACTGAGATGAGGCCAGC
SNEV (Δ U90) sense	GTAGAATTCACCTCTGCGCCAGCAGCTG
SNEV 56 sense	GTAGAATTCAAAGTTGCTCACCCAAATCCG
SNEV 66 sense	GTAGAATTCCTCAGCCACCAGCATCCC
SNEV 76 sense	GTAGAATTCAAAGCTTTGCAGGATGAGTG
SNEV 92 antisense	ATACAAGTCGACGCTGTCAGCTGTGGCGCAG
SNEV 103 antisense	ATACAAGTCGACTGGTACAGAGCGTGTGAC AG
SNEV 121 antisense	ATACAAGTCGACGACGAGTACTTCTTGGT

Capital letters represent nucleotides complementary to the template, underlined letters specify restriction sites, Kozak consensus sequences are in italic and additional initiation- and termination triplets are in bold letters.

All constructs were sequence analyzed before transformation into yeast or transfection into HeLa cells. The expression plasmid containing SNEV for expression in the insect cell/baculovirus system was kindly provided by Prof. Hatakeyama.

Growth, sporulation and forward mutability

Transformed yeast clones were tested for growth at 30 and 37°C on SD agar plates, for their ability to sporulate at 30°C on KAC agar plates and for mutability on Canavanine containing media as described (10).

Antibody production and affinity purification

Synthetic peptides were designed from the protein sequence of SNEV, synthesized and antibodies raised against them were purified commercially (Eurogentec, Belgium). Peptide sequences used for antibody production were as follows: SNEV-865: 33-YIAENGTDPINNQPL-S-48, SNEV-866: 185-TERKKRGKTVPEELV-C-199; SNEV-867: 336-QTG-RVLT KVTDETSV-C-350. The antisera were affinity purified against the peptides used to raise the antibodies (Eurogentec). Affinity purified antibodies were dialyzed against phosphate-buffered saline (PBS) containing 0.02% sodium azide and stored at -80°C.

Monoclonal antibodies to SNEV were produced using a novel FACS based technique and after recombinant expression purified from culture supernatants using Protein A agarose beads (37).

SDS-PAGE and western blotting

SDS-PAGE gel analysis was done as described previously (38). For protein expression analysis of the transformed MG5128 yeast strain, lysis was performed using 1 ml breaking buffer [50 mM sodium phosphate (pH 7.4), 1 mM phenylmethylsulfonyl fluoride (PMSF), 1 mM EDTA and 5% glycerol] in a French press at 1500 psi. For immunoblotting, the washed immunoprecipitates were resuspended in 50 µl of 2× SDS-PAGE loading buffer and heat denatured at 95°C for 5 min. A total of 10–15 µl of the samples were loaded on a 10% SDS-PAGE gel or on a 4–12% pre-cast gradient gel (NOVEX). The separated proteins were transferred on to Hybond-C extra membrane (Amersham Pharmacia Biotech) by electroblotting. The membranes carrying the transferred proteins were blocked with 5% non-fat milk powder and 0.3% Tween-20 in PBS, or with 3% BSA and 0.3% Tween-20 in PBS, for His-tagged proteins. The membranes were incubated with primary antibody for 1 h at room temperature, washed with blocking buffer and incubated with the appropriate secondary antibody. The primary antibodies were used at the following dilutions: anti-TetraHis (Qiagen) (1:5000), rabbit anti-SNEV-867 and -866 (1:1000), mouse monoclonal anti-SNEV (1:2000), anti-CDC5L (1:1000). After washing the blots in blocking buffer 3–4 times (5 min per wash at room temperature), the membranes were incubated with a secondary antibody coupled to horseradish peroxidase (HRP). Protein bands were detected by developing blots using the ECL or ECL-plus kit (Amersham Pharmacia Biotech).

Yeast two-hybrid assays

Screening for SNEV interacting proteins was performed using the MATCHMAKER GAL4 Two-Hybrid System3 (Clontech

Laboratories, Palo Alto, USA) according to the manufacturer's guidelines. The plasmids were introduced into *S.cerevisiae* strain AH109 (Clontech Laboratories, Palo Alto, USA) by LiAc-cotransformation. As prey library we used the Matchmaker Aorta cDNA library (Clontech Laboratories, Palo Alto, USA). We selected interaction-positive clones by growth on high stringency synthetic drop out medium (4× SD: -Trp/-Leu/-His/-Ade). Plasmids were prepared from yeast as described and sequence analyzed.

GST pull-down assay

The pGEX-6P-1 plasmid containing the GST-SNEV cDNA was transformed into *E.Coli* BL21. The fusion protein was expressed using Overnight Express Autoinduction System 1 (Novagen, Darmstadt, Germany) and purified using the Micro Spin GST Purification Module (Amersham Biosciences, Uppsala, Sweden) according to the manufacturer's protocol. His₆-SNEV was expressed in Sf9 insect cells, and affinity purified on a Ni²⁺-NTA column as described (37). For the pull-down assay, equal amounts of the purified proteins (0.5 µg) were mixed together and incubated for 2 h at 4°C in CoIP-buffer [200 mM NaCl, 25 mM Tris-HCl (pH 7.4) and 0.5% Triton]. Glutathione sepharose 4B beads (Amersham Biosciences, Uppsala, Sweden), equilibrated with CoIP-buffer, were added and followed by incubation for 2 h at 4°C. The beads were washed 3 times with CoIP-buffer, and proteins were eluted with SDS-PAGE sample buffer. After SDS-PAGE, co-precipitated SNEV was detected using anti-4His antibody (Qiagen, Hilden, Germany). GST was probed using a goat anti-GST antibody (Amersham, Uppsala, Sweden) and an anti-goat peroxidase conjugate used as secondary antibody (Sigma-Aldrich, St. Louis, USA) for ECL detection. For competition assays we added synthetic peptides to 0.5 µg GST-SNEV and again used Glutathione sepharose 4B beads (Amersham Biosciences, Uppsala, Sweden), equilibrated with CoIP-buffer, to pull-down GST-SNEV. After 3 washes with CoIP-buffer, proteins were eluted with SDS-PAGE sample buffer, and detected by western blotting.

Cell culture and transfection

HeLa cells were grown in DMEM supplemented with 10% fetal calf serum (FCS) and 100 U/ml penicillin and streptomycin (Life Technologies, Inc.). For immunofluorescence assays, cells were grown on coverslips and transfected using Effectene transfection reagent (Qiagen) according to the manufacturer's instructions.

Cell staining and immunofluorescence analyses

Cells were washed in PBS and fixed for 5 min in 3.7% (w/v) para-formaldehyde in CSK buffer [10 mM PIPES (pH 6.8), 10 mM NaCl, 300 mM sucrose, 3 mM MgCl₂ and 2 mM EDTA] at room temperature (RT). Permeabilization was performed with 1% Triton X-100 in PBS for 15 min at RT. Cells were incubated with primary antibodies diluted in PBS with 1% goat serum for 35 min to 1 h at RT, washed 3 times for 10 min with PBS, incubated for 35 min to 1 h at RT with the appropriate secondary antibodies diluted in PBS with 1% goat serum, and washed 3 times for 10 min with PBS. Antibodies used were Y12 monoclonal antibody (anti-Sm) (dilution

1:500), rabbit anti-CDC5L (1:500) and rabbit anti-SNEV-867 (1:100).

Microscopy and image analysis was carried out using a Zeiss DeltaVision Restoration microscope as described previously (39).

FRET

SNEV and SNEV Δ 98 inserted in pECFP-C1 and pEYFP-C1, respectively were transiently co-transfected into HeLa cells by effectene reagent (Qiagen) according to the manufacturer's guidelines. After 24 h FRET images from living cells were generated by the MicroFRET method according to Youvan (40). Photos were captured on a Nikon Diaphot TMD microscope with a cooled charge coupled device camera (Kappa GmbH, Gleichen, Germany), with the YFP, CFP and FRET filter sets (Omega Optical Inc., Brattleboro, USA), under identical conditions and processed with Scion Image software version beta 4.0.2 (Scion Corp., Frederick, USA). The images were aligned by pixel shifting, inverted and background was subtracted. Images from the YFP and CFP filter sets were multiplied with their previously assessed correction factors (0.19 for YFP and 0.59 for CFP) and subtracted from the FRET filter set picture. The remaining signal was multiplied for better visualization and represents the corrected FRET.

In vitro splicing assay and native gels

Nuclear extracts used in the splicing assays were obtained commercially from Computer Cell Culture Center (Mons, Belgium). Splicing assays were done using uniformly labelled, capped pre-mRNAs incubated with nuclear extract as described previously (41). Recombinant proteins were added to the splicing reactions. The adeno-pre-mRNA was transcribed from *Sau3AI*-digested plasmid pBSAd1 (42). The splicing reactions were loaded on a 10% polyacrylamide, 8 M urea denaturing gel and run in 1 \times TBE to separate the splicing products. When samples were to be used for the analysis of splicing complexes, the reactions were loaded on to a polyacrylamide-agarose composite gel (43) and run for about 5 h at 25 mA.

RESULTS

SNEV shows sequence homology and similar domain architecture to the yeast splicing factor Prp19p

After identifying SNEV as differentially expressed between early passage and senescent cells (1), we were interested in determining the possible functions of this protein. In order to detect putative functional motifs of SNEV sensitive sequence analysis methods were applied and resulted in the detection of the following sequence segments (Figure 1A): a U-box domain hit from the SMART (1–68, *E*-value < 10⁻²⁸; possible role in E2 dependent ubiquitination processes), a moderately polar low complexity region (91–101), a putative coiled coil segment (114–135), a highly charged region (10 positive, 6 negative out of 34 amino acid from 175–208), and a large G β -like domain containing 7 WD40 repeats in accordance with PFAM, SMART and REP hits (210–504, *E*-values between 10⁻¹² and 10⁻¹). Yet another, possibly globular domain (136–174) did not show any consensus to functional domains.

Sequence database searches reveal close full-length sequential homologues in *Rattus norvegicus* (BAA95215), *Drosophila melanogaster* (AAD46846), *Caenorhabditis elegans* (Q10051), *Arabidopsis thaliana* (two different hits AAB80652 and AAB70423), *Plasmodium falciparum* (T18432), *Saccharomyces pombe* (O14011) and also to *S.cerevisiae* (Prp19p). Although sequence similarity is very high only in the N-terminal region (Figure 1B), the domain architecture of SNEV and Prp19p is similar throughout the whole protein sequence (Figure 1A).

Prp19p is an essential protein for *S.cerevisiae*, and has already been shown in several studies to play an important role in splicing and DNA repair. Therefore, we tried to complement a yeast Prp19p mutant strain with human SNEV or with different human–yeast chimeric constructs.

A SNEV/Prp19p chimeric protein restores wild-type phenotype in a temperature sensitive Prp19p mutant strain

The Prp19p mutant yeast strain MG5128 (pso4-1) was transformed with plasmid constructs containing various wild-type and chimeric proteins in order to test restoration of the wild-type phenotype regarding temperature sensitivity, UV resistance, forward mutability and sporulation. The summarized results are shown in Figure 2A. Positive transformants were selected by the nutritional marker URA at the permissive temperature of 30°C and analyzed for expression of the His₆-tagged proteins by western blotting, which was confirmed for all transformants (Figure 2B). By incubation of the transformed yeast strains at 37°C the potential of the recombinant SNEV chimera to complement temperature sensitivity was assessed (Figure 2C). Empty vector control did not result in growth of MG5128 at the restrictive temperature, while yeast overexpressing wild-type Prp19p including a C-terminal His₆-tag were able to divide at 37°C, indicating that the C-terminal His₆-tagged protein is functional. Overexpression of the pso4-1 derived Prp19p mutant protein that carries a point mutation leading to substitution of the highly conserved leucine at position 45 by serine (L45S) complemented the temperature sensitivity as well. No other mutation in the promoter or terminator sequence was observed (data not shown).













Prp19 without the U-box (Prp19[68–503], construct f in Figure 2A) as well as SNEV[1–66]Prp19[68–503] (construct e) were able to complement the defects of MG5128, indicating that the U-box is not necessary for complementation in the background of the MG5128 mutant strain.

Furthermore, the human–yeast chimeric protein SNEV [1–91]Prp19[98–503] (construct g) restores wild-type phenotype in contrast to its control, the N-terminal deletion of 97 amino acids, Prp19[98–503] (construct h), indicating that the amino acids from position 68 to 97 are of major importance for the function of SNEV and Prp19p.

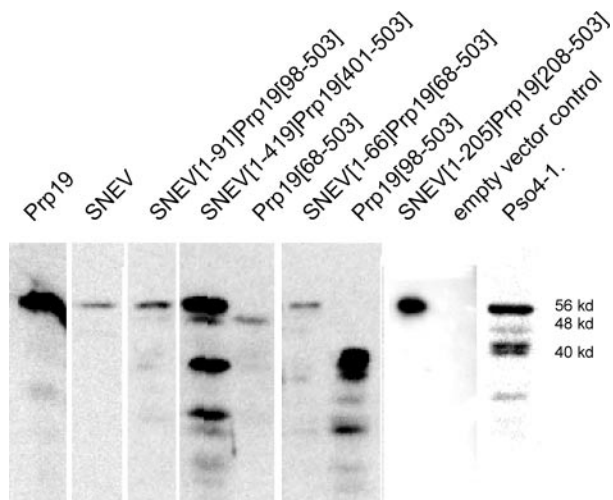
None of the other chimeric constructs (i–l) was able to complement MG5128, however, wild-type SNEV negatively affected yeast growth suggesting that competition with the yeast protein occurs (data not shown).

The same constructs that were effective for enabling growth at the restrictive temperature restored the wild-type behaviour when we tested the ability to sporulate on KAC agar plates

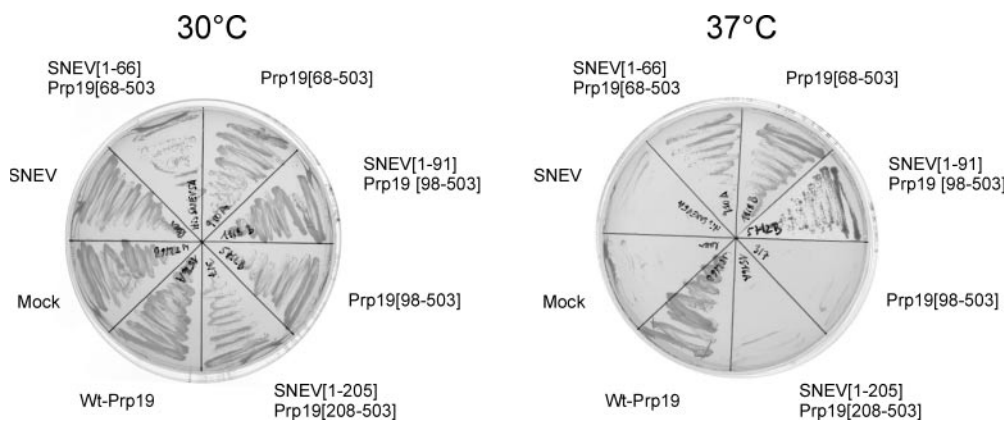
A

	Construct	Graphic	Length MW	Growth 30°C	Growth 37°C	Sporulation	Forward mutability
a	SNEV		504 aa 56 kd	+	---	---	---
b	His ₆ -wtPrp19		503 aa 56 kd	+++	---	n.d.	n.d.
c	wtPrp19-His ₆		503 aa 56 kd	+++	+++	+++	+++
d	Pso4-1 derived PRP19-His ₆		503 aa 56 kd	+++	+++	+++	+++
e	SNEV[1-66]Prp19[68-503]-His ₆		501 aa 55 kd	+++	+++	+++	+++
f	Prp19[68-503]-His ₆		436 aa 48 kd	+++	+++	+++	+++
g	SNEV[1-91]Prp19[98-503]-His ₆		497 aa 54 kd	+++	+++	+++	+++
h	Prp19[98-503]-His ₆		407 aa 45 kd	+++	---	---	---
i	SNEV[1-205]Prp19[208-503]-His ₆		501 aa 55 kd	+++	---	---	---
j	Prp19[208-503]-His ₆		296 aa 32 kd	+++	---	---	---
k	SNEV[1-420]Prp19[401-503]-His ₆		522 aa 57 kd	+++	---	---	---
l	Prp19[401-503]-His ₆		103 aa 11 kd	+++	---	---	---

B



C



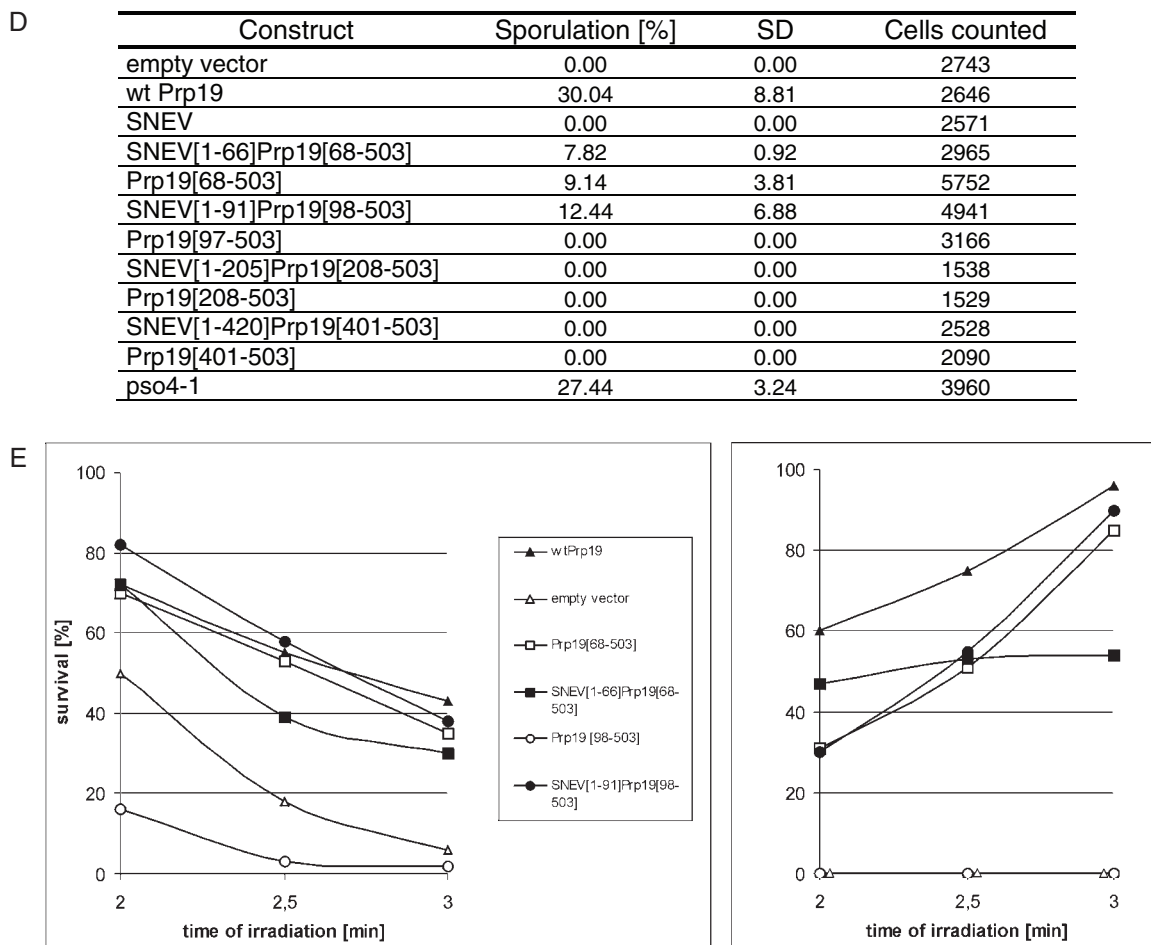


Figure 2. Human–yeast chimeric SNEV complements the mutant phenotype of MG5128. **(A)** Overview of SNEV and Prp19 constructs tested in this study. Length indicates the number of amino acids (aa), MW is the molecular weight (kd), (+) indicates ability to grow at the indicated temperature, to sporulate or to perform forward mutability. (–) no growth, (n.d.) not determined. The star in construct d indicates the point mutation. **(B)** All chimeric constructs introduced into the mutant yeast strain are translated into protein. Western blots after SDS–PAGE of cell-lysates of MG5128 transformed with pYPG15, containing various chimeric constructs, which were fused to a His₆-tag. Detection was performed using anti-TetraHis mouse antibody as primary and peroxidase-conjugated goat-anti-mouse antibody as secondary antibody. Calculated molecular masses [kDa] are indicated. The small bands in lanes 4–6 and 11–14 represent degradation products resulting from the lysis process. **(C)** Growth at the permissive (30°C) and the non-permissive (37°C) temperature of MG5128, transformed with the various constructs was analysed. All clones showed growth at 30°C, whereas at 37°C only transformants containing wtPrp19p, SNEV[1–66]Prp19p[68–503], Prp19p[68–503] or SNEV[1–91]Prp19p[98–503] were able to form colonies. Sector 1: wt Prp19p (positive control), 2: empty vector control, 3: SNEV, 4: SNEV[1–66]Prp19p[68–503], 5: Prp19p[68–503], 6: SNEV[1–91]Prp19p[98–503], 7: Prp19p[97–503], 8: SNEV[1–205]Prp19p[208–503]. **(D)** Ability of the various constructs to sporulate on KAC agar plates. MG5128 transformed with the various constructs was incubated at 30°C for one week, vegetative and sporulated cells were counted. Sporulation was calculated as the ratio of sporulated versus vegetative cells. Mean and standard deviation (SD) were calculated from at least three independent experiments. The total number of cells counted is indicated. **(E)** The human–yeast chimeric protein SNEV[1–66]Prp19[68–503] restores wild-type phenotype regarding UV sensitivity and forward mutability. Survival of the various MG5128 transformants after UV-irradiation (left panel) (266 nm) and ability of the various chimeric constructs to restore wild-type like forward mutability by growth on canavanine containing media after UV-irradiation (right panel). Number of mutants has been calculated as mutants per UV radiation surviving cells.

(Figure 2D) and the ability to restore forward mutability and resistance to UV radiation (Figure 2E). All results and constructs are summarized in Figure 2A. These data suggest that SNEV might have the same cellular function as Prp19p, however, further analysis of SNEV's role during the splicing process was necessary for conclusive interpretation.

SNEV colocalizes with splicing factors in HeLa cell nuclei

Since SNEV appears to be related to Prp19p both at the structural and functional level, we decided to investigate if

the protein has a role in human pre-mRNA splicing. We tested in indirect immunofluorescence experiments whether endogenous SNEV associates with known human splicing factors in the cell nucleus and localizes to nuclear structures called 'speckles', where several other pre-mRNA splicing factors accumulate. We transiently expressed a fluorescently tagged SNEV fusion protein in HeLa cells and stained with anti-SNEV antibodies to check if the tagged protein accumulates in the same nuclear structures as endogenous SNEV (Figure 3A). We next investigated SNEV's association with other splicing factors in HeLa cell nuclei. The results from these experiments indicate that the protein colocalizes within

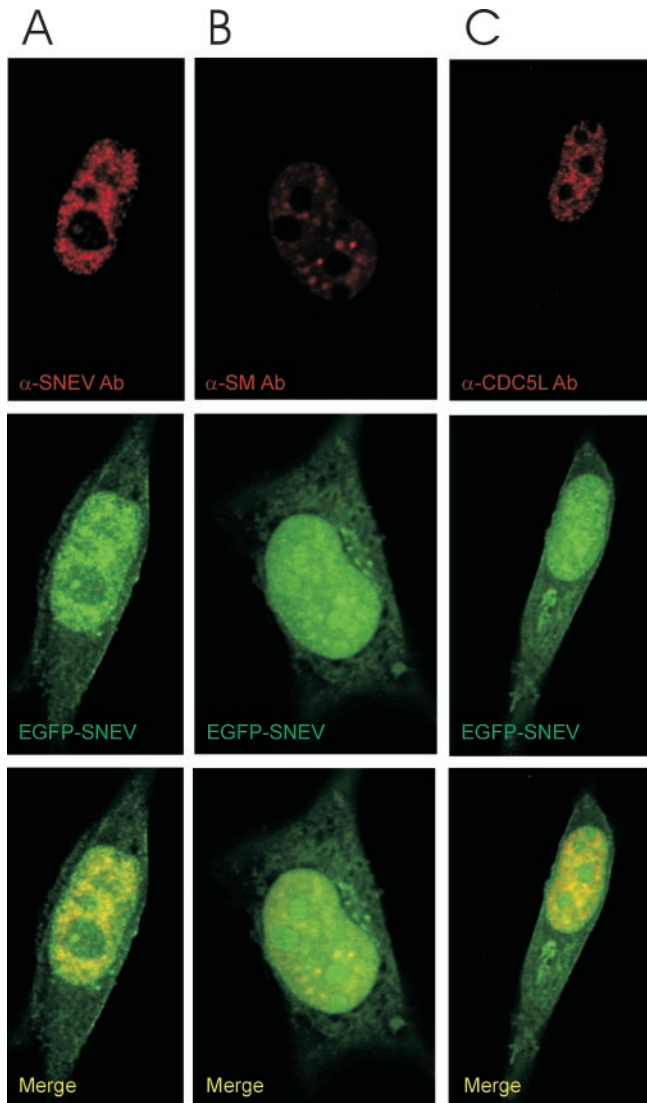


Figure 3. SNEV associates *in vivo* with Sm proteins as well as with the splicing factor CDC5L, and fusion of SNEV to EGFP does not alter the cellular localization of SNEV. HeLa cells were grown, transfected with an EGFP-SNEV fusion construct, fixed and stained by indirect immunofluorescence. The images shown in the panels are representative optical sections from the respective deconvolved datasets. (A) GFP-SNEV expressing HeLa cells stained with anti-SNEV antibody 867. Red represents SNEV indirect staining, and green indicates EGFP-SNEV expression. (B) Cells were stained with the anti-Sm protein monoclonal antibody Y12 (57). Red indicates Y12 staining as above, while green represents EGFP-SNEV expression. (C) Cells stained with anti-CDC5L antibodies. Red represents anti-CDC5L staining, while green shows EGFP-SNEV expression. In all the panels, yellow indicates co-localization of the two proteins. Note that the use of the fluorescently labelled protein results in a stronger signal from the fusion protein. This shows up as a small fraction of the label that does not co-localize.

the nucleus with other human splicing factors, namely Sm proteins as detected by the Y12 antibody (Figure 3B) and CDC5L (44) (Figure 3C). Colocalization in nuclear speckles is observed in all cases.

SNEV is an essential human splicing factor

Since SNEV associates with other splicing factors in cells, we tested if the presence of SNEV in nuclear extracts is

essential for the splicing reaction. Therefore, we performed immunodepletion experiments. Since it has been shown previously that SNEV is part of the CDC5L associated complex (19), we used high salt concentrations in the nuclear extracts to disrupt this complex before depletion. After removing the NaCl by dialysis, the extracts were tested for splicing efficiency. The SNEV immunodepleted nuclear extracts showed a reduction in splicing activity. No reduction of splicing efficiency was observed when various control antibodies were used in immunodepletion experiments (Figure 4A). Since add back of cytoplasmic extract S100, that also contains SNEV (data not shown) restores the splicing efficiency, we were able to exclude the possibility that unspecific inhibition due to sample processing had occurred. Addition of recombinantly expressed SNEV in increasing amounts, however, did not restore splicing activity; on the contrary, complete inhibition of the reaction was observed. The success of SNEV immunodepletion was monitored by western blotting. Indeed, nuclear extracts contained significantly less SNEV after depletion, when compared to the controls that were treated with IgG and α -HCF antibodies. However, when we tested, if 1 M NaCl was sufficient to disrupt the CDC5L complex, we probed the immunoprecipitates also positive for the presence of CDC5L. This co-depletion of CDC5L together with SNEV from the nuclear extracts indicates a very high stability of the CDC5L associated complex. Thus, it is comprehensible that add back of recombinant SNEV is not sufficient to restore splicing activity. But why do we see complete inhibition of splicing by recombinant SNEV?

The inhibition of the splicing reaction seems to take place at the step of spliceosome assembly, since we observed that addition of increasing amounts of recombinant SNEV to SNEV-depleted as well as untreated nuclear extracts leads to inhibition of spliceosome formation as seen on native gels, while no block in spliceosome assembly is seen when equimolar amounts of another His-tagged protein is added (Figure 5A). This is not due to decreased stability of the spliceosome by heparin (data not shown). Additionally, we observed that already formed spliceosomes are not disrupted upon addition of SNEV at different time points (from 0 to 50 min) during the reaction, indicating that assembled spliceosomes are protected against the disruptive activity (Figure 5B). These data again argue in favour of a role of SNEV in the splicing reaction, however, proof of a direct role of SNEV escaped due to the high stability of the CDC5L complex.

SNEV forms homo-oligomers

Additional help in clarifying the role of SNEV came from our project that aims at the identification of SNEV interacting proteins using yeast two-hybrid screening. Thereby, we identified several potential SNEV interacting proteins as well as SNEV itself. Figure 6A shows colony formation of yeast after co-transformation with SNEV as bait and prey protein. In order to map the interaction site we co-transformed various truncated SNEV mutants together with full length SNEV. Only mutants containing the amino acids 68–90 gave rise to colonies on high stringency medium. Furthermore, we were able to show that a minimal region containing amino acid 56 to 92 (Mut 1) or 56 to 121 (Mut 4) is not only necessary but also sufficient to mediate SNEV self interaction, while

neither 66–103 (Mut 2) nor 76–121 (Mut 3) allowed yeast colony formation on 4× drop out medium (Figure 6C). This would suggest that the binding site lies between amino acid positions 56 and 66, however, it cannot be excluded that these 10 amino acids are only necessary for correct

formation of an interaction site lying within the amino acids from 66 to 92.

As an independent method confirming direct SNEV–SNEV interaction *in vitro*, we performed GST pull-down assays using recombinant His-tagged and GST-tagged SNEV (Figure 6D). GST–SNEV was recombinantly expressed in *E.coli*, while His-tagged SNEV was derived from insect cells and affinity purified on Ni-NTA agarose beads (37). Neither the beads nor GST alone precipitated the His-tagged SNEV, but it was efficiently pulled down by GST–SNEV. These results suggest that SNEV-fusion proteins interact directly *in vitro* (Figure 6D). When we tested the synthesized peptide Prp19-1 spanning the region from 56 to 74 as competitor for SNEV–SNEV interaction in the GST pull-down experiment, the amount detected by western blots decreased significantly, while the control peptide Prp19-scr consisting of the scrambled sequence did not reduce the precipitated amount of GST–SNEV (Figure 6E). The reduction of precipitated SNEV decreases also in a dose dependent manner (Figure 6F). This indicates that the peptide efficiently competes with SNEV self interaction.

An additional indication that SNEV interacts with itself derives from FRET experiments. By using ECFP and EYFP tagged SNEV we observed significant FRET signals, while the negative control using EYFP-SNEV and ECFP–SNEVΔ98 lacking the interaction site did not produce any significant FRET signals (Figure 6G). Although the FRET experiment does not allow localizing the interaction within the cell, these results still indicate that SNEV–SNEV self interactions may exist in HeLa cells *in vivo*.

Synthetic peptides containing sequences in the self-interaction domain inhibit pre-mRNA splicing

Since the region from 56 to 94 was sufficient to bind SNEV in the Y2H system and to compete with the SNEV–SNEV interaction in GST pull-down experiments, we decided to investigate whether peptides containing sequences in this self-interaction domain of SNEV will compete with the endogenous protein for binding and thus interfere with SNEV's function in splicing. We therefore used peptides containing the following sequences present in the self-interaction

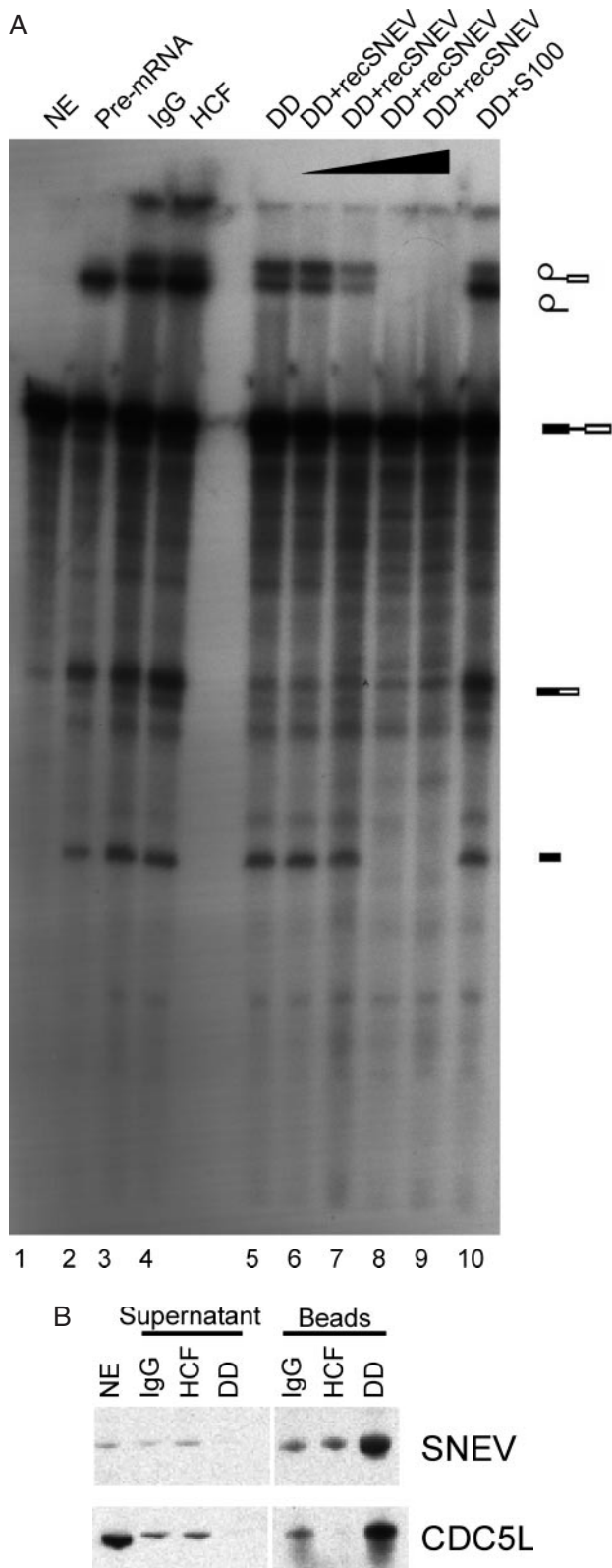


Figure 4. Depletion of SNEV decreases the splicing efficiency of nuclear extracts. (A) After immunodepletion of SNEV from nuclear extracts (NE) treated with 1 M NaCl in order to disrupt the CDC5L complex the extracts were tested for splicing efficiency. Lane 1 shows the unspliced adenoviral pre-mRNA. A decrease of the second catalytic step of the reaction was observed in the SNEV depleted extracts when compared to depleted controls, where irrelevant antibodies were used for depletion (lanes 3 and 4) or where untreated NE was used for *in vitro* splicing (lane 2). Splicing efficiency is restored, when S100 cytoplasmic extract enriched for splicing factors is added to the SNEV depleted NE (lane 10). However, add back of increasing amounts of recombinant SNEV results in concentration dependent inhibition of the first step of the reaction (lanes 6–9). (B) The antibody used to immunodeplete the high salt nuclear extracts recognizes a distinct band at the expected molecular weight of 56 kDa in nuclear extract (lane NE). While neither IgG nor an irrelevant antibody reduce the amount of SNEV in the nuclear extracts used in the splicing assay after immunodepletion, a marked decrease in SNEV was observed after depletion with α -SNEV antibody. This is consistent with the larger amounts that are eluted from the α -SNEV antibody coupled beads. Although 1 M NaCl was used to disrupt the CDC5L associated complex, CDC5L was co-precipitated together with SNEV. Supernatant: Nuclear extracts after immunodepletion. Beads: Precipitates eluted from the beads. NE (nuclear extract), IgG: IgG coupled beads, HCF: α -HCF antibody coupled beads, DD: α -SNEV antibody coupled beads.

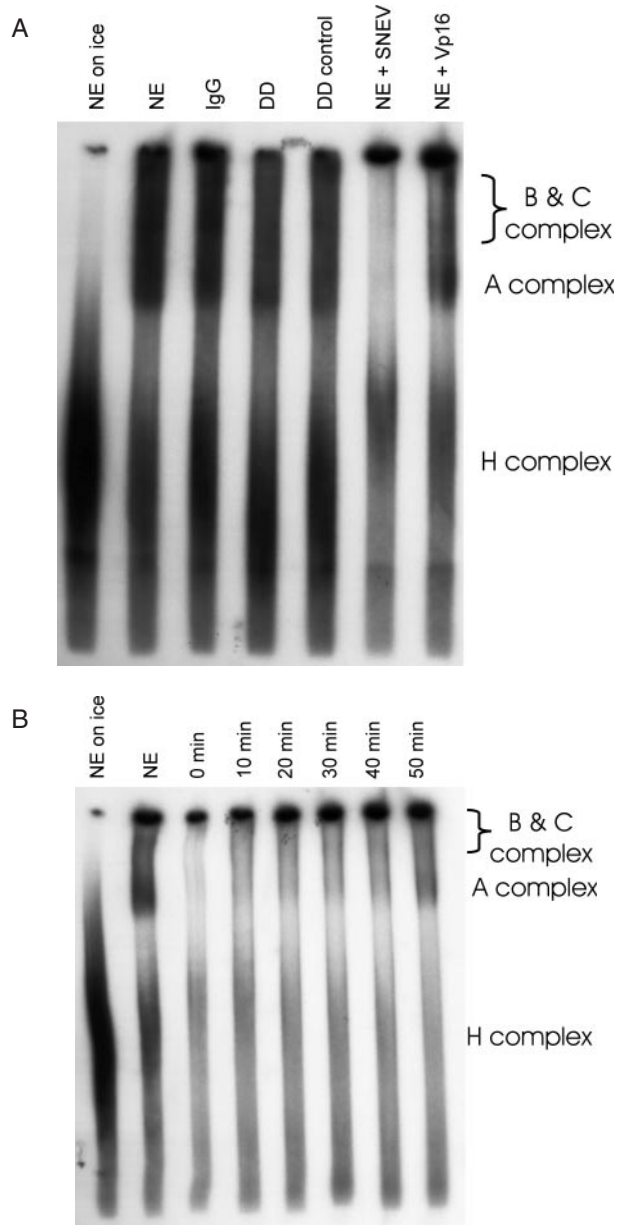


Figure 5. SNEV inhibits spliceosome formation, but does not disrupt already formed complexes. (A) Formation of the splicing complexes was observed by separation on native gels. Lane 1: nuclear extract (NE) on ice as negative control, lane 2: nuclear extract, lane 3: NE after treating with pre-immune IgG coupled beads, lane 4: NE after SNEV depletion, lane 5: NE after treating with anti-SNEV coupled beads pre-incubated with recombinant His₆-SNEV, lane 6: NE after addition of recombinant His₆-SNEV, lane 7: NE after addition of the same amount of recombinant His₆-VP16 proteins as control. Immunodepletion of SNEV only slightly decreases formation of the spliceosome, while after addition of recombinant SNEV no splicing complexes can be detected. (B) Already formed complexes are not disrupted by addition of SNEV in a time course experiment. Lane 1: NE on ice, lane 2: NE, lane 3: NE with SNEV added before starting the reaction, lane 4: SNEV was added 10 min after starting of the reaction, lane 5: 20 min; lane 6: 30 min, lane 7: 40 min, lane 8: 50 min after starting the reaction.

domain: Prp19-1 (56-KVAHPIRPKPPSATSIPAI-74), Prp19-2: (75-LKALQDEWDAVMLHSFTL-92), Prp19-3: (66-PSATSIPAILKALQDEWDA-84) and Prp19-4: (56-KVAHPIRPKPPSATSIPAILKALQDEWDAVMLHSFTL-92). As a control we used Prp19-scr, a scrambled version of Prp19-1

(N-KSIAATSPIPVRKIHPAP-C). Upon addition of these peptides, we observed that splicing can be inhibited when either Prp19-1 or PRP19-4 is added to the splicing reaction whereas the peptides Prp19-2 and -3 did not block splicing (Figure 7A). In order to define the potency of Prp19-1 and Prp19-4 we used increasing amounts of these peptides in comparison to the scrambled version of Prp19-1 as negative control. While Prp19-1 inhibited the splicing reaction completely at about 14 nmol, about 21 nmol of Prp19-4 were needed to show the same effect. Neither concentration of the scrambled peptide showed a decrease in splicing efficiency (Figure 7B). These results indicate that the SNEV sequences represented by the inhibitory peptides are essential for the proteins function in splicing.

Inhibition of splicing by Prp19-1 peptide is due to a decrease in spliceosome stability

In order to find out whether the splicing inhibition observed above is due to a specific inhibition of splicing catalysis or spliceosome assembly, we next investigated the effect of the peptides on spliceosome assembly. Splicing reactions were prepared as above except that the reactions were loaded on to a native gel at the end of the reaction in order to separate the splicing complexes. The results obtained from these experiments indicate that the inhibitory peptide Prp19-1 prevents formation of splicing complexes whereas the control peptide does not block assembly of the spliceosome (Figure 7C). It is of note that the larger peptide Prp19-4 that blocks catalysis at higher concentrations does not block spliceosome formation. It is possible that Prp19-1 has higher affinity to SNEV than the larger Prp19-4 peptide. However, it is also possible that SNEV interaction is inside of the complex and only the smaller Prp19-1 is able to disrupt the SNEV self interaction, while the larger peptide is sterically blocked from the interaction site. More experiments are needed to address the differences between the effects of the peptides.

However, addition of Prp19-1 at different time points, starting with a pre-incubation of nuclear extracts for 10 min up to addition just before loading of the gel, showed, that already formed complexes are disrupted by Prp19-1, while Prp19-scr as negative control has no effect. These results suggest that SNEV-SNEV self interaction may be needed for the efficient formation and stability of splicing complexes. Although most members of the Prp19 associated complex have been found to enter the spliceosome just before catalysis, SNEV has been observed to be already present in the A complex (45).

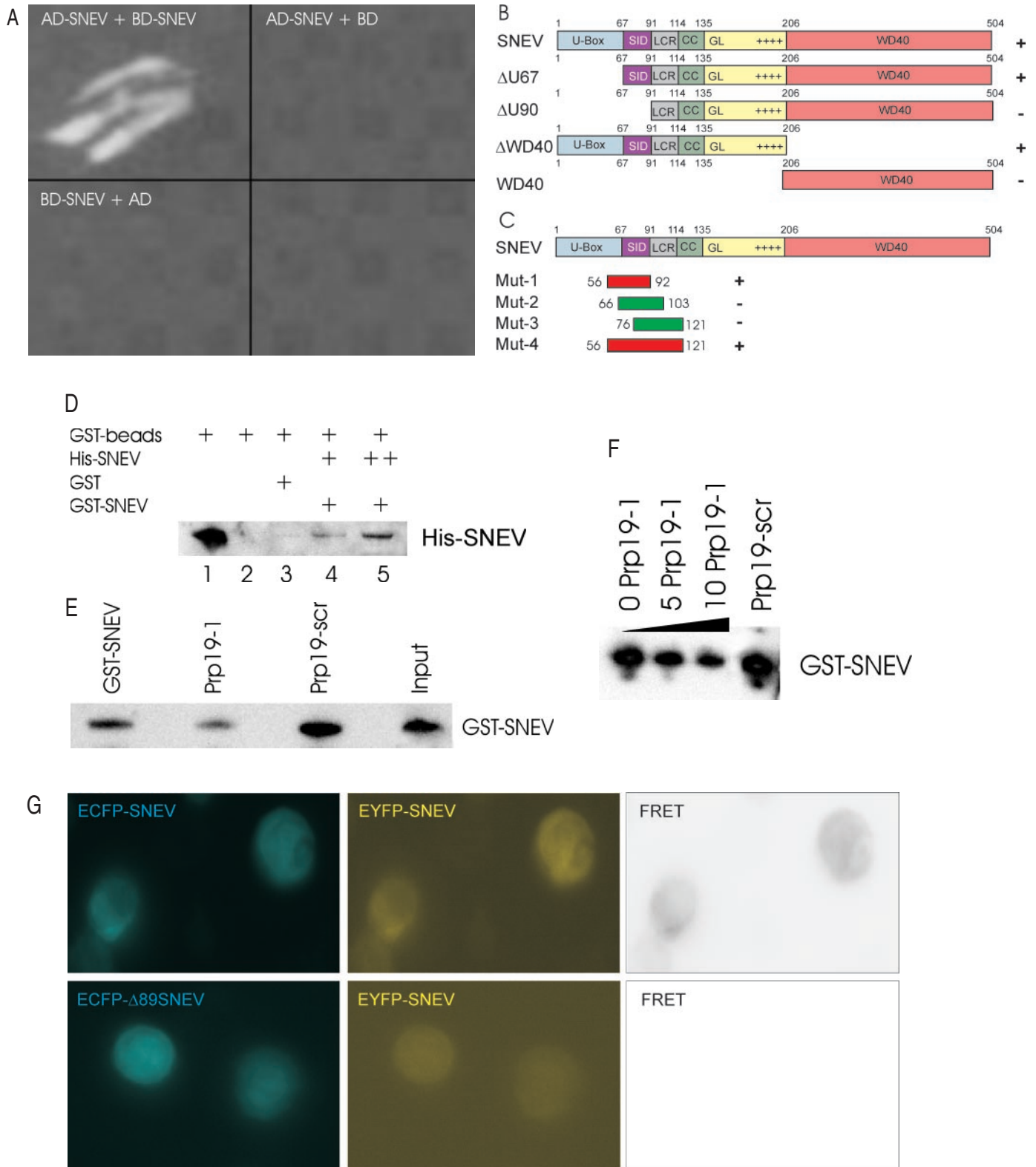
Additionally these results might help to explain the cause of the inhibitory effect of adding recombinant SNEV to splicing reactions. Although this recombinant SNEV was active in ubiquitination assays (data not shown), the recombinant protein might not be active as a splicing factor and thus might compete with the binding sites in endogenous SNEV similarly to the inhibitory peptide.

DISCUSSION

By a subtractive hybridization method various differentially expressed genes were identified from early passage and senescent HUVECs (1). One of these genes, the unknown gene 4, now termed SNEV, was selected for further characterization.

Sequence analysis of SNEV revealed 5 putative domains, a domain architecture that is highly similar to the one found for the yeast Prp19p protein (46). The C-terminal portion of SNEV contains 7 WD40 repeats that are similar to Gβ-like

proteins. WD40 repeats have a typical length of about 40 residues, form a β-propeller structure, and are proposed to mediate protein–protein interactions (47). WD40 motifs are also a common motif in F-box proteins and E3 ligase



complexes (48). The putative SNEV coiled coil region represents another segment with protein–protein interaction ability (49).

Within the first 68 amino acids a U-box (a modified RING finger) domain was found by SMART search. This conserved domain is found in a large variety of proteins (50) and possibly mediates the interaction of the U-box protein with ubiquitin conjugated proteins thus activating their further multi-ubiquitination by acting as E4 ubiquitin ligase enzymes (51). *In vitro* assays by Hatakeyama and coworkers (17) have shown that SNEV possesses an E3 ubiquitin ligase activity when tested with Ubc3 (cdc34) acting as an E2 enzyme, and the ubiquitination has been suggested to be dependent on the U-box. Additionally, SNEV mediates multi-ubiquitination via the K48 residue, which is known to be the proteasome targeting signal (52,53). Recently we observed that SNEV also interacts with the proteasome, suggesting that it ‘escorts’ its substrate to the site of destruction (18).

Since the putative yeast homologue of SNEV, Prp19p, has been well characterized, but shows only limited sequence homology (23%) we next tested if SNEV or SNEV–Prp19 chimeric proteins are able to complement the pleiotropic defects of the yeast mutant strain pso4-1. This mutant strain, MG5128, shows a highly interesting phenotype including temperature sensitivity, blocked sporulation and impaired mutability (10) as well as an accumulation of pre-mRNA at the restrictive temperature (14).

Here we have shown that a chimeric protein containing the human U-box and adjacent 30 amino acids (SNEV[1–91]Prp19p[98–503]) restores the wild-type phenotype, in contrast to its control, where only the Prp19p part (Prp19p[98–503]) was introduced. Since the chimeric protein consisting of the 205 human N-terminal amino acids fused to the Prp19p WD40 repeat domain (construct i) was not effective, at least 91, but not more than 204 human N-terminal amino acids, will restore the wild-type yeast phenotype.

Equally effective in restoring wild-type properties of pso4-1 was the truncated Prp19p lacking the U-box (Prp19p[68–503]) that we had designed as a control. This result is surprising in several regards: (i) the mutation of MG5128 was found within the U-box itself at the highly conserved leucine at position 45 (50), and no other mutation neither in the promoter nor the terminator sequence was observed (data not shown), (ii) overexpression of the mutant protein results in complete

restoration of the defects of MG1528 (construct d), (iii) the U-box is essential for viability in Prp19p null yeast (46). Therefore we suggest that the mutation of L45 results in a destabilization of the Prp19p structure not only in the U-box, but also in the adjacent regions.

Expression of human SNEV in the mutant yeast strain resulted in diminished growth rates even at the permissive temperature of 30°C, indicating that it competes with Prp19p most probably by its N-terminus, since the human C-terminal part cannot substitute for the function of the C-terminal part of Prp19p. This is consistent with our result that constructs carrying parts of the human WD40 domain cannot complement the yeast mutant.

Taken together, the results of the yeast complementation experiments suggest that at least the N-terminal part of SNEV can complement Prp19p function and therefore SNEV might be its functional orthologue. Prp19p is a known yeast splicing factor, therefore if SNEV is a functional homologue of the yeast protein, it should function in pre-mRNA splicing in human cells. Immunostaining and cDNA cell transfection experiments show that SNEV colocalizes with well known splicing factors like Sm proteins and CDC5L in HeLa cell nuclei. These results suggest that SNEV may function in splicing and confirm previous observations that indicate an association of SNEV with the human CDC5L associated splicing factor complex (19).

We next investigated the potential for a direct role of SNEV in human pre-mRNA splicing by immunodepleting the protein from HeLa nuclear extracts. The results from these experiments indicate that removing SNEV from nuclear extracts prevents the formation of splicing products. Even though we performed the depletion from nuclear extracts treated with high salt concentrations, we still co-depleted CDC5L. Although these results confirm the importance of the CDC5L associated complex for *in vitro* splicing reactions, the question still remained, whether or not SNEV alone is an essential splicing factor in human cells.

A result from a different line of experiments helped us to address this question. By using yeast two-hybrid screenings to identify SNEV interacting proteins, we observed that the protein interacts with itself. The interaction was confirmed using GST pull-down assays as well as by FRET experiments and subsequently, the interaction site was narrowed down to 30 amino acids. Synthetic peptides covering these amino

Figure 6. SNEV forms homo-oligomers that are dependent on the amino acids 56–92 of SNEV. (A) SNEV interacts with SNEV in a yeast two-hybrid assay when GAL4-AD-SNEV and GAL4-BD-SNEV are co-transformed into the yeast reporter strain AH109 (AD-SNEV + BD-SNEV). Neither co-transformation of SNEV fusion to the GAL4 activating domain (AD-SNEV + BD) nor to the DNA-binding domain (BD-SNEV + AD) together with the respective empty second plasmid allowed formation of yeast colonies on high stringency drop-out media plates. (B) Domain mapping of the self interacting amino acids was performed using the Yeast two-hybrid system. Various truncated SNEV constructs were used as prey. Growth of double transformants on high stringency media plates was observed only for variants containing amino acids 68–90, which we therefore termed self interaction domain (SID). (C) In order to confirm that the SID is sufficient for homo-oligomerization, four small overlapping peptides were cloned and tested by Y2H. Co-transformation with SNEV resulted in growth of yeast double transformants on high stringency media plates only with the region 56–92 and 56–121 (red), while neither 66–103 nor 76–121 (green) allowed yeast colony formation. U-box: domain necessary for ubiquitin E3 ligase activity of SNEV; SID: Self Interaction domain; LCR: low complexity region; GL2: globular domain 2, WD40: domain containing 7 WD40 repeats; numbers indicate the amino acid positions, ‘+’ indicates colony formation on high stringency drop out media, ‘–’ indicates no colony formation. (D) The SNEV self-interaction was confirmed by GST pull-down experiments using affinity purified His₆-SNEV and GST-SNEV. While no His₆-SNEV was detectable in the controls using either GST or beads alone (lanes 2 and 3), GST-SNEV results in co-precipitation of His₆-SNEV (lanes 4 and 5). (E) Addition of Prp19-1 peptide to GST-SNEV reduces the amount of precipitated SNEV (Prp19-1), whereas addition of the scrambled control peptide (Prp19-scr) does not. This amount is comparable to the one without addition of peptides (GST-SNEV) as well as to the amount of GST-SNEV added to the beads (Input). (F) Increasing amounts of the Prp19-1 peptide (0, 5 and 10 nM) decrease the amount of precipitated GST-SNEV (G) Additional confirmation of SNEV self interaction derives from FRET analysis. Upper panel: Co-transfection of ECFP-SNEV and EYFP-SNEV into HeLa cells resulted. Pictures were taken using CFP-filter (ECFP-SNEV) displayed in cyan, YFP-filter (EYFP-SNEV). FRET represents the calculated net FRET signal. Lower panel: negative control using ECFP-SNEVΔ98 lacking the interaction domain.

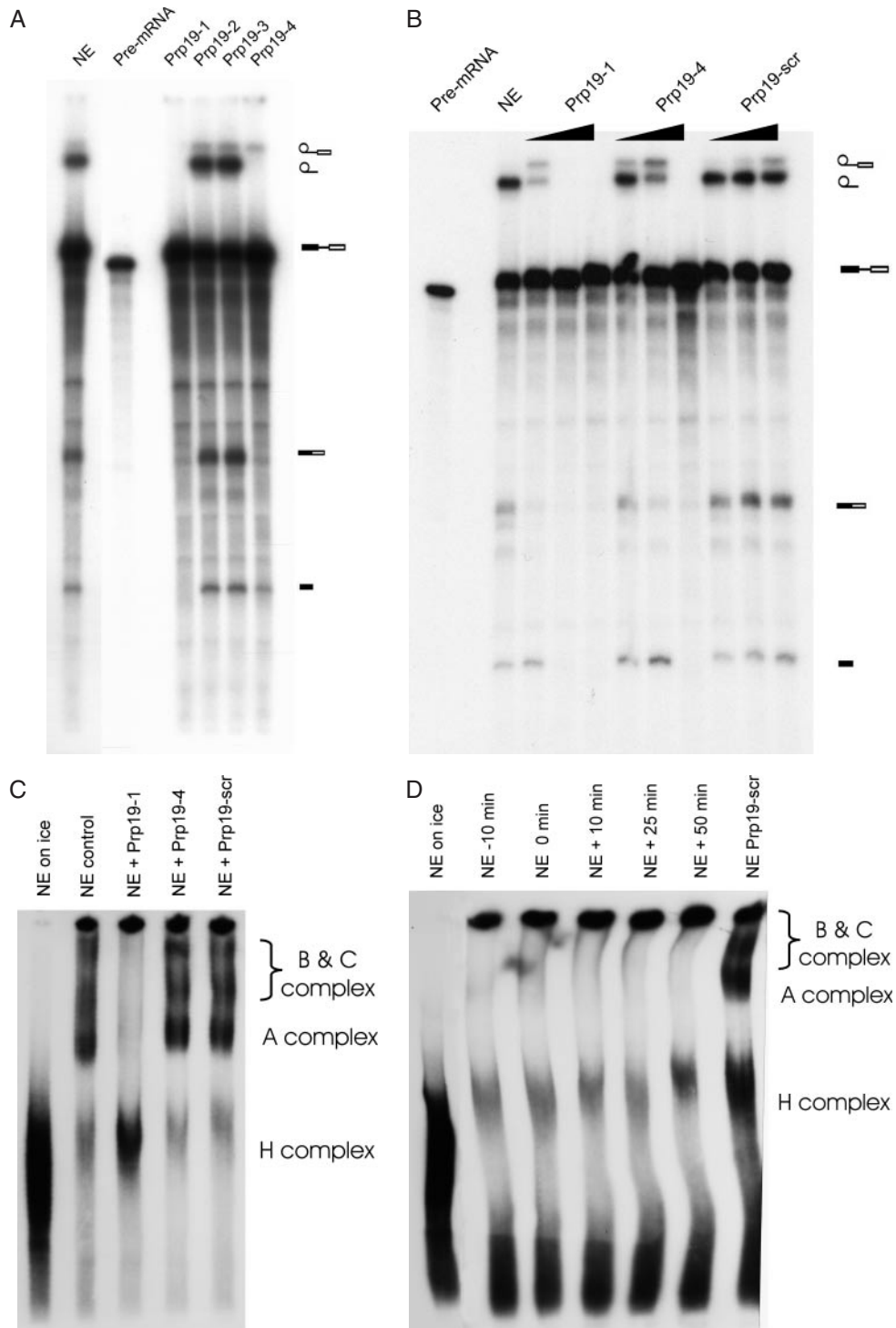


Figure 7. A peptide that spans the SNEV self interaction site inhibits the splicing reaction by interfering with spliceosome stability. **(A)** Overlapping peptides that span the self interaction site of SNEV were synthesized and added to standard splicing reactions. While nuclear extract (NE) as positive control shows efficient splicing of an adenoviral pre-mRNA, the peptides Prp19-1 and Prp19-4 show inhibition of the splicing reaction, while Prp19-2 and Prp19-3 do not affect formation of lariat and of joined exons. **(B)** Increasing amounts (7, 14 and 21 nmol) of the two effective peptides were added to the splicing reaction, showing higher potency for Prp19-1 than for Prp19-4. As negative control the same amounts of Prp19-scr, the scrambled version of Prp19-1 was used. **(C)** Splicing complexes have been separated on a native gel. Addition of Prp19-1 (NE + Prp19-1) peptide results in inhibition of formation of C, B and A splicing complexes similar to incubation of the splicing reaction on ice (NE on ice), while Prp19-4 (NE + Prp19-4) as well as Prp19-scr (NE + Prp19-scr) similar to the positive control (NE) do not show any reduction in spliceosome assembly. **(D)** 21 nmol Prp19-1 were added to splicing reactions at different time points: either pre-incubation for 10 min (–10 min), at the start of the reaction (0 min), or at 10 min, 25 min and 50 min after starting the splicing reaction. After 55 min all reactions were loaded on to native gels. Neither A, B nor C complexes can be detected independent from the time point of peptide addition, while the scrambled peptide does not interfere with spliceosome formation.

acid sequences were synthesized and used as competitors of the SNEV–SNEV interaction. Indeed, less SNEV was ‘pulled down’ in the presence of increasing amounts of Prp19-1 peptide, indicating that the SNEV–SNEV interaction is inhibited by the peptide *in vitro*.

Addition of these peptides to *in vitro* splicing experiments blocks pre-mRNA splicing. Similar results were obtained previously by targeting the interaction of two other CDC5L associated proteins CDC5L and PRLG1 by synthetic peptides (54). While these peptides interfered with splicing catalysis, addition of the Prp19-1 peptide interfered with spliceosome assembly. This finding is supported by the observation that SNEV joins the human spliceosome as early as at the pre-spliceosome stage (45), indicating that a role of SNEV in early spliceosome assembly is possible. Although we cannot rule out entirely that Prp19-1 has effects on other splicing factors as well, the competitive GST pull-down assay strongly supports a specific function on endogenous SNEV. We further suggest that SNEV might act as a scaffold on which the other splicing factors assemble, covering SNEV at the inside of this complex. This would be in keeping with the finding that recombinant SNEV prevents spliceosome assembly but does not disrupt the already formed complexes, while the small Prp19-1 peptide is able to disrupt also the fully assembled spliceosomes. Prp19-4, while still efficiently inhibiting the splicing reaction at higher concentrations, might have lower affinity or sterical disadvantage and might therefore not be able to prevent spliceosome assembly or disrupt already formed spliceosomes. However, further experiments are necessary to explain the observed differences in the capacity to disrupt the spliceosome.

While addition of recombinant SNEV in excess inhibits splicing *in vitro*, 2- to 3-fold overexpression extends the life span of endothelial cells (2). This seemingly contradictory result might be explained that recombinant SNEV is not correctly folded and therefore competing with the endogenous SNEV in nuclear splicing extracts, or by the excess added *in vitro* that might titrate other necessary factors, while stable SNEV overexpressing cells generate fully functional SNEV, that besides its function as splicing factor has also DNA protective functions (55) and increases stress resistance of endothelial cells (2).

Consistent with our results, the self-interaction domain of yeast Prp19p was also mapped by Ohi and coworkers (56) to the amino acids from 66 to 141. Disruption of the tetramerization of Prp19p was achieved by mutating the highly conserved W88 to proline, which was lethal in a Prp19p null background, while a change to alanine did not interfere with self interaction or with yeast viability.

Considering that Prp19p and SNEV are orthologues and show high conservation as well as exchangeability in the N-terminal region in our complementation experiments, these results might indicate that although the region 54–74 is sufficient for self interaction, the adjacent amino acids play a crucial role for accessibility of this region as shown by the W88P mutation. This might also explain why the L45S mutation was complemented by Prp19 Δ 1–67. The mutated form might destabilize the Prp19p associated complex, while it can form properly without the N-terminal 67 amino acids (as shown by our domain mapping). Therefore

the pleiotropic phenotype of the L45S mutation might not only derive from an altered activity of the U-box, but also from a decreased complex stability.

In summary, our results together with already published data suggest that SNEV is the orthologue of Prp19 and has been highly conserved during evolution. Both proteins show similar domain architecture despite low sequence similarity at the C-terminal half. They both carry a U-box which *in vitro* shows E3 ubiquitin ligase activity (17,46), both proteins interact with the proteasome (18), both have been reported to play a role in DNA repair (10,55), and both are subunits of a highly conserved complex (termed NTC in yeast and CDC5L associated complex in human cells), which is essential for splicing. It will be very interesting to understand how these multiple functions are integrated into cellular pathways and how splicing, DNA repair and the ubiquitin proteasome pathway are interrelated.

ACKNOWLEDGEMENTS

We are grateful to Polymun Scientific, Vienna for generously funding of this project and to the Österreichische Forschungsgemeinschaft for funding a stay of J.G. in Dundee. Furthermore this work is supported by the Austrian Science fund, NRN grant S093-06. We thank Gerhard Adam for yeast expression plasmids and discussion as well as Johannes Schmid for help with FRET analysis. F.E. was supported by Boehringer Ingelheim. Funding to pay the Open Access publication charges for this article was provided by University of Natural Resources and Applied Life Sciences.

Conflict of interest statement. None declared.

REFERENCES

1. Grillari, J., Hohenwarter, O., Grabherr, R.M. and Katinger, H. (2000) Subtractive hybridization of mRNA from early passage and senescent endothelial cells. *Exp. Gerontol.*, **35**, 187–197.
2. Voglauer, R., Chang, M., Wieser, M., Dampier, B., Baumann, K., Schreiber, M., Katinger, H. and Grillari, J. Overexpression of SNEV extends the replicative life span of human endothelial cells. *Exp. Cell Res.*, in press.
3. Tarn, W.Y., Lee, K.R. and Cheng, S.C. (1993) Yeast precursor mRNA processing protein PRP19 associates with the spliceosome concomitant with or just after dissociation of U4 small nuclear RNA. *Proc. Natl Acad. Sci. USA*, **90**, 10821–10825.
4. Tarn, W.Y., Hsu, C.H., Huang, K.T., Chen, H.R., Kao, H.Y., Lee, K.R. and Cheng, S.C. (1994) Functional association of essential splicing factor(s) with PRP19 in a protein complex. *EMBO J.*, **13**, 2421–2431.
5. Chen, H.R., Jan, S.P., Tsao, T.Y., Sheu, Y.J., Banroques, J. and Cheng, S.C. (1998) SNT309p, a component of the Prp19p-associated complex that interacts with Prp19p and associates with the spliceosome simultaneously with or immediately after dissociation of U4 in the same manner as Prp19p. *Mol. Cell. Biol.*, **18**, 2196–2204.
6. Chen, H.R., Tsao, T.Y., Chen, C.H., Tsai, W.Y., Her, L.S., Hsu, M.M. and Cheng, S.C. (1999) Snt309p modulates interactions of Prp19p with its associated components to stabilize the Prp19p-associated complex essential for pre-mRNA splicing. *Proc. Natl Acad. Sci. USA*, **96**, 5406–5411.
7. Chen, C.H., Tsai, W.Y., Chen, H.R., Wang, C.H. and Cheng, S.C. (2001) Identification and characterization of two novel components of the Prp19p-associated complex, Ntc30p and Ntc20p. *J. Biol. Chem.*, **276**, 488–494.
8. Tsai, W.Y., Chow, Y.T., Chen, H.R., Huang, K.T., Hong, R.I., Jan, S.P., Kuo, N.Y., Tsao, T.Y., Chen, C.H. and Cheng, S.C. (1999) Cef1p is a

- component of the Prp19p-associated complex and essential for pre-mRNA splicing. *J. Biol. Chem.*, **274**, 9455–9462.
9. Ohi, M.D. and Gould, K.L. (2002) Characterization of interactions among the Cef1p-Prp19p-associated splicing complex. *RNA*, **8**, 798–815.
 10. Grey, M., Dusterhoft, A., Henriques, J.A. and Brendel, M. (1996) Allelism of PSO4 and PRP19 links pre-mRNA processing with recombination and error-prone DNA repair in *Saccharomyces cerevisiae*. *Nucleic Acids Res.*, **24**, 4009–4014.
 11. de Moraes, M.A. Jr, Vicente, E.J., Brozmanova, J., Schenberg, A.C. and Henriques, J.A. (1996) Further characterization of the yeast *pso4-1* mutant: interaction with *rad51* and *rad52* mutants after photoinduced psoralen lesions. *Curr. Genet.*, **29**, 211–218.
 12. Henriques, J.A. and Moustacchi, E. (1980) Isolation and characterization of *pso* mutants sensitive to photo-addition of psoralen derivatives in *Saccharomyces cerevisiae*. *Genetics*, **95**, 273–288.
 13. Henriques, J.A., Vicente, E.J., Leandro da Silva, K.V. and Schenberg, A.C. (1989) PSO4: a novel gene involved in error-prone repair in *Saccharomyces cerevisiae*. *Mutat Res.*, **218**, 111–124.
 14. Revers, L.F., Cardone, J.M., Bonatto, D., Saffi, J., Grey, M., Feldmann, H., Brendel, M. and Henriques, J.A. (2002) Thermoconditional modulation of the pleiotropic sensitivity phenotype by the *Saccharomyces cerevisiae* PRP19 mutant allele *pso4-1*. *Nucleic Acids Res.*, **30**, 4993–5003.
 15. Brendel, M. and Henriques, J.A. (2001) The *pso* mutants of *Saccharomyces cerevisiae* comprise two groups: one deficient in DNA repair and another with altered mutagen metabolism. *Mutat Res.*, **489**, 79–96.
 16. Gotzmann, J., Gerner, C., Meissner, M., Holzmann, K., Grimm, R., Mikulits, W. and Sauermann, G. (2000) hNMP 200: a novel human common nuclear matrix protein combining structural and regulatory functions. *Exp. Cell Res.*, **261**, 166–179.
 17. Hatakeyama, S., Yada, M., Matsumoto, M., Ishida, N. and Nakayama, K.I. (2001) U box proteins as a new family of ubiquitin-protein ligases. *J. Biol. Chem.*, **276**, 33111–33120.
 18. Löscher, M., Fortschegger, K., Ritter, G., Wostry, M., Voglauer, R., Schmid, J.A., Watters, S., Rivett, A.J., Ajuh, P., Lamond, A.I. *et al.* (2005) The U-box E3 ligase SNEV interacts with the 7 subunit of the 20S proteasome. *Biochem J.*, **388**, 593–603.
 19. Ajuh, P., Kuster, B., Panov, K., Zomerdijk, J.C., Mann, M. and Lamond, A.I. (2000) Functional analysis of the human CDC5L complex and identification of its components by mass spectrometry. *EMBO J.*, **19**, 6569–6581.
 20. Makarov, E.M., Makarova, O.V., Urlaub, H., Gentzel, M., Will, C.L., Wilm, M. and Luhrmann, R. (2002) Small nuclear ribonucleoprotein remodeling during catalytic activation of the spliceosome. *Science*, **298**, 2205–2208.
 21. Makarova, O.V., Makarov, E.M., Urlaub, H., Will, C.L., Gentzel, M., Wilm, M. and Luhrmann, R. (2004) A subset of human 35S U5 proteins, including Prp19, function prior to catalytic step 1 of splicing. *EMBO J.*, **23**, 2381–2391. Epub 2004 Jun 23.
 22. Staley, J.P. and Guthrie, C. (1998) Mechanical devices of the spliceosome: motors, clocks, springs, and things. *Cell*, **92**, 315–326.
 23. Will, C.L. and Luhrmann, R. (1997) Protein functions in pre-mRNA splicing. *Curr. Opin. Cell Biol.*, **9**, 320–328.
 24. Chan, S.P., Kao, D.I., Tsai, W.Y. and Cheng, S.C. (2003) The *prp19p*-associated complex in spliceosome activation. *Science*, **302**, 279–282.
 25. Villa, T. and Guthrie, C. (2005) The Isy1p component of the NineTeen complex interacts with the ATPase Prp16p to regulate the fidelity of pre-mRNA splicing. *Genes Dev.*, **19**, 1894–1904.
 26. Gornemann, J., Kotovic, K.M., Hujer, K. and Neugebauer, K.M. (2005) Cotranscriptional spliceosome assembly occurs in a stepwise fashion and requires the cap binding complex. *Mol. Cell*, **19**, 53–63.
 27. Wootton, J.C. and Federhen, S. (1996) Analysis of compositionally biased regions in sequence databases. *Methods Enzymol.*, **266**, 554–571.
 28. Lupas, A. (1997) Predicting coiled-coil regions in proteins. *Curr. Opin. Struct. Biol.*, **7**, 388–393.
 29. Claros, M.G. and von Heijne, G. (1994) TopPred II: an improved software for membrane protein structure predictions. *Comput. Appl. Biosci.*, **10**, 685–686.
 30. Brendel, V., Bucher, P., Nourbakhsh, I.R., Blaisdell, B.E. and Karlin, S. (1992) Methods and algorithms for statistical analysis of protein sequences. *Proc. Natl Acad. Sci. USA*, **89**, 2002–2006.
 31. Bateman, A., Birney, E., Durbin, R., Eddy, S.R., Howe, K.L. and Sonnhammer, E.L. (2000) The Pfam protein families database. *Nucleic Acids Res.*, **28**, 263–266.
 32. Schultz, J., Copley, R.R., Doerks, T., Ponting, C.P. and Bork, P. (2000) SMART: a web-based tool for the study of genetically mobile domains. *Nucleic Acids Res.*, **28**, 231–234.
 33. Andrade, M.A., Ponting, C.P., Gibson, T.J. and Bork, P. (2000) Homology-based method for identification of protein repeats using statistical significance estimates. *J. Mol. Biol.*, **298**, 521–537.
 34. Altschul, S.F., Madden, T.L., Schäffer, A.A., Zhang, J., Zhang, Z., Miller, W. and Lipman, D.J. (1999) Gapped BLAST and PSI-BLAST: a new generation of protein database search programs. *Nucleic Acids Res.*, **25**, 3389–3402.
 35. Sambrook, J. and Russell, D.W. (2001) *Molecular Cloning: A Laboratory Manual*. Cold Spring Harbor Laboratory Press, Cold Spring Harbor.
 36. Gietz, D., St. Jean, A., Woods, R.A. and Schiestl, R.H. (1992) Improved method for high efficiency transformation of intact yeast cells. *Nucleic Acids Res.*, **20**, 1425.
 37. Böhm, E., Grillari, J., Gross, S., Ernst, W., Ferko, B., Borth, N. and Kättinger, H. Monoclonal antibodies against SNEV by a novel FACS technique. *J. Immunol. Meth.*, in press.
 38. Laemmli, U.K. (1970) Cleavage of structural proteins during the assembly of the head of bacteriophage T4. *Nature*, **227**, 680–685.
 39. Platani, M., Goldberg, I., Swedlow, J.R. and Lamond, A.I. (2000) *In vivo* analysis of Cajal body movement, separation, and joining in live human cells. *J. Cell Biol.*, **151**, 1561–1574.
 40. Youvan, D.C., Silva, C.M., Bylina, E.J., Coleman, W.J., Dilworth, M.R. and Yang, M.M. (1997) Calibration of fluorescence resonance energy transfer in microscopy using genetically engineered GFP derivatives on nickel chelating beads. *Biotech et alia*, **3**, 1–18.
 41. Lamond, A.I., Konarska, M.M. and Sharp, P.A. (1987) A mutational analysis of spliceosome assembly: evidence for splice site collaboration during spliceosome formation. *Genes Dev.*, **1**, 532–543.
 42. Konarska, M.M. and Sharp, P.A. (1987) Interactions between small nuclear ribonucleoprotein particles in formation of spliceosomes. *Cell*, **49**, 763–774.
 43. Konarska, M.M. and Sharp, P.A. (1986) Electrophoretic separation of complexes involved in the splicing of precursors to mRNAs. *Cell*, **46**, 845–855.
 44. Ajuh, P., Sleeman, J., Chusainow, J. and Lamond, A.I. (2001) A direct interaction between the carboxyl-terminal region of CDC5L and the WD40 domain of PLRG1 is essential for pre-mRNA splicing. *J. Biol. Chem.*, **276**, 42370–42381.
 45. Hartmuth, K., Urlaub, H., Vornlocher, H.P., Will, C.L., Gentzel, M., Wilm, M. and Luhrmann, R. (2002) Protein composition of human prespliceosomes isolated by a tobramycin affinity-selection method. *Proc. Natl Acad. Sci. USA*, **99**, 16719–16724.
 46. Ohi, M.D., Vander Kooi, C.W., Rosenberg, J.A., Chazin, W.J. and Gould, K.L. (2003) Structural insights into the U-box, a domain associated with multi-ubiquitination. *Nature Struct. Biol.*, **10**, 250–255.
 47. van der Voorn, L. and Ploegh, H.L. (1992) The WD-40 repeat. *FEBS Lett.*, **307**, 131–134.
 48. Kipreos, E.T. and Pagano, M. (2000) The F-box protein family. *Genome Biol.*, **3002.1–3002.7**.
 49. Kammerer, R.A. (1997) Alpha-helical coiled-coil oligomerization domains in extracellular proteins. *Matrix Biol.*, **15**, 555–565; discussion 567–558.
 50. Aravind, L. and Koonin, E.V. (2000) The U box is a modified RING finger - a common domain in ubiquitination [letter]. *Curr. Biol.*, **10**, R132–r134.
 51. Koegl, M., Hoppe, T., Schlenker, S., Ulrich, H.D., Mayer, T.U. and Jentsch, S. (1999) A novel ubiquitination factor, E4, is involved in multiubiquitin chain assembly. *Cell*, **96**, 635–644.
 52. Ciechanover, A. and Schwartz, A.L. (1998) The ubiquitin-proteasome pathway: the complexity and myriad functions of proteins death. *Proc. Natl Acad. Sci. USA*, **95**, 2727–2730.
 53. Weissman, A.M. (2001) Themes and variations on ubiquitylation. *Nature Rev. Mol. Cell Biol.*, **2**, 169–178.
 54. Ajuh, P. and Lamond, A.I. (2003) Identification of peptide inhibitors of pre-mRNA splicing derived from the essential interaction domains of CDC5L and PLRG1. *Nucleic Acids Res.*, **31**, 6104–6116.
 55. Mahajan, K.N. and Mitchell, B.S. (2003) Role of human Pso4 in mammalian DNA repair and association with terminal deoxynucleotidyl transferase. *Proc. Natl Acad. Sci. USA*, **100**, 10746–10751.

56. Ohi, M.D., Vander Kooi, C.W., Rosenberg, J.A., Ren, L., Hirsch, J.P., Chazin, W.J., Walz, T. and Gould, K.L. (2005) Structural and functional analysis of essential pre-mRNA splicing factor Prp19p. *Mol. Cell. Biol.*, **25**, 451–460.
57. Pettersson, I., Hinterberger, M., Mimori, T., Gottlieb, E. and Steitz, J. (1984) The structure of mammalian small nuclear ribonucleoproteins. Identification of multiple protein components reactive with anti-(U1)ribonucleoprotein and anti-Sm autoantibodies. *J. Biol. Chem.*, **259**, 5907–5914.